Electronic Supplementary Information

Multifunctional, robust sponges by a simple adsorption-combustion method

Yu Yang, Zhenjun Liu, Jian Huang and Chaoyang Wang*

Research Institute of Materials Science
South China University of Technology, Guangzhou, 510640, China
E-mail: zhywang@scut.edu.cn

Movie S1. Self-cleaning test. In the movie, hydrophobic SiO_2 nanoparticles were evenly scattered on an inclined UHF sponge surface simulating the dirt particles. Soon afterwards, water droplets were dropped on the surface, and the sponge surface exhibited excellent self-cleaning property with all of the SiO_2 nanoparticles washed out.

Movie S2. Absorption test. In the movie, a piece of USF sponge was applied to absorb hexane (dyed with Sudan I) which was floating on the water.

Movie S3. Squeezing test. In the movie, a piece of UHF sponge was applied to absorb and recovery gasoline (dyed with Sudan I) which was mixed with water via an absorption/squeezing cycling method.

Table S1 Elements and their contents of different sponges.

Samples	C (wt %)	O (wt %)	N (wt %)	Fe (wt %)	Ni (wt %)
Original sponge	7	31	62	-	-
UHF sponge	12	26	62	-	-
UHF sponge after distillation	13	27	60	-	-
UHF sponge after combustion	12	21	67	-	-
UHF sponge after squeezing	12	24	64	-	-
Magnetic UHF sponge	8	20	33	39	-
Ni foam	-	2	-	-	98
Carbon-deposited Ni foam	9	3	-	-	88

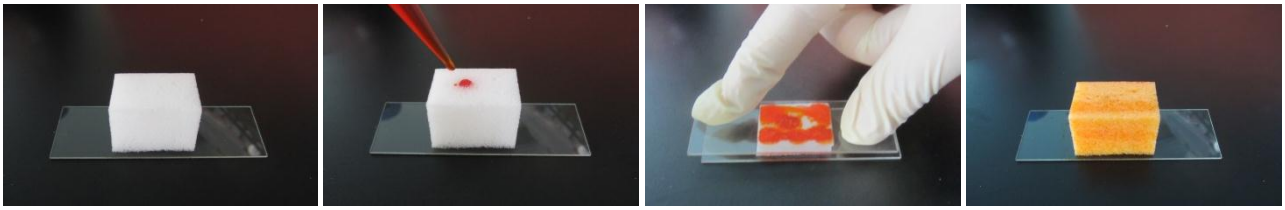

Fig. S1. The PMF sponge was wetted by toluene (dyed by Sudan I) by an absorb-compress-release cycle process. The toluene-absorbed sponge was compressed from different direction to ensure the toluene could homogeneously distribute in the sponge.

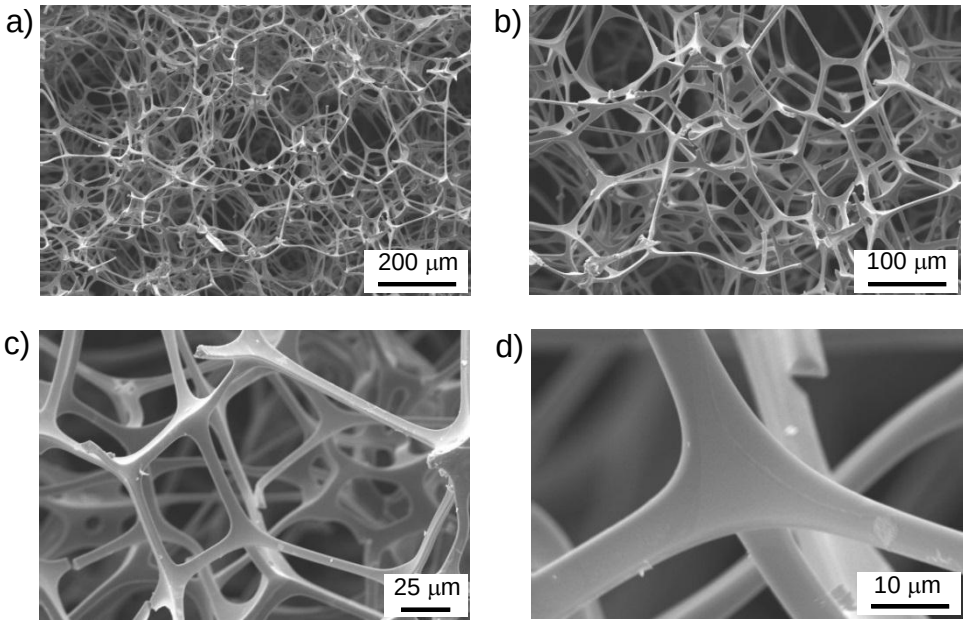

Fig. S2. The SEM images of the original PMF sponges in different magnifications. The skeleton of the sponge exhibits with smooth surface. The structure possesses pore of about 100-200 μm and the skeleton diameter is about 5-10 μm.

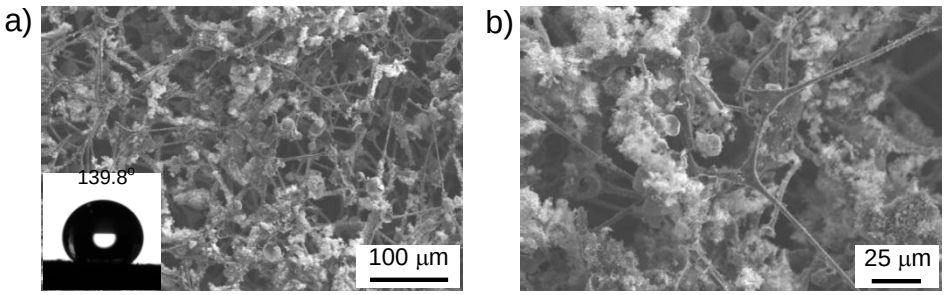

Fig. S3. Different magnification SEM images of the sponges fabricated using xylene as carbon sources. It was revealed that the obtained sponge did not consisted of the similar micaro-nanoscale hierarchical porous structure of the UHF sponge which was synthesized based on toluene. At the same time, the water contact angle reduced to 139.8^{o}.

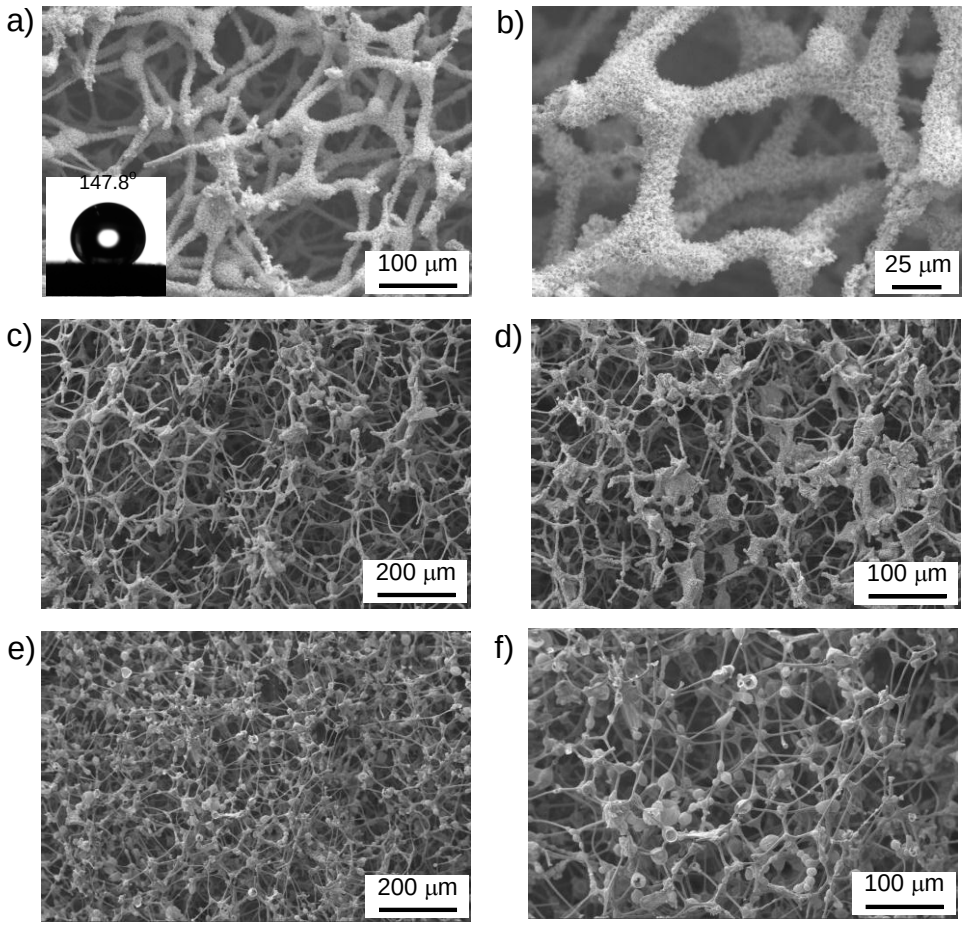

Fig. S4. (a) and (b) are different magnification SEM images of the sponges fabricated using benzene as carbon sources. It was showed that the obtained sponge consisted of the similar micaro-nanoscale hierarchical porous structure of the UHF sponge which was synthesized based on toluene. At the same time, the water contact angle was 147.8^{o}. (c) and (d) are different magnification SEM images of sponges using alcohol as carbon sources. (e) and (f) are different magnification SEM images of sponges using n-hexane as carbon sources.

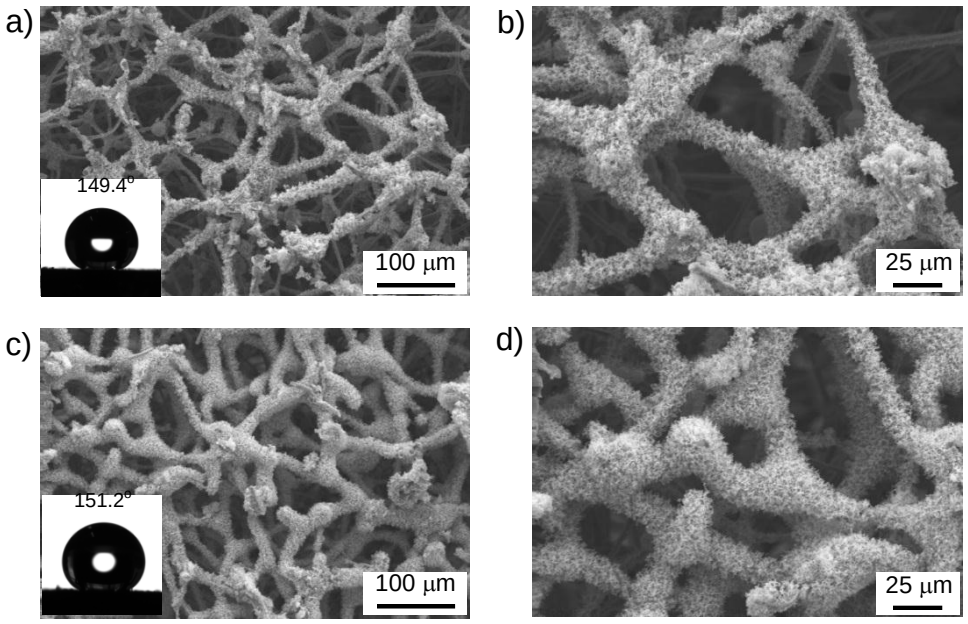

Fig. S5. SEM images of sponges fabricated based on different amount of toluene: (a) and (b) 25 mg toluene per cm^3; (c) and (d) 50 mg toluene per cm^3. Micaro-nanoscale hierarchical porous structure could be obtained in both kinds of sponges. In addition, the water contact angle of them turned out to be 149.4^o and 151.2^o. Increasing the amount of the toluene had little effect on the structure and surface wettability of the obtained architecture.

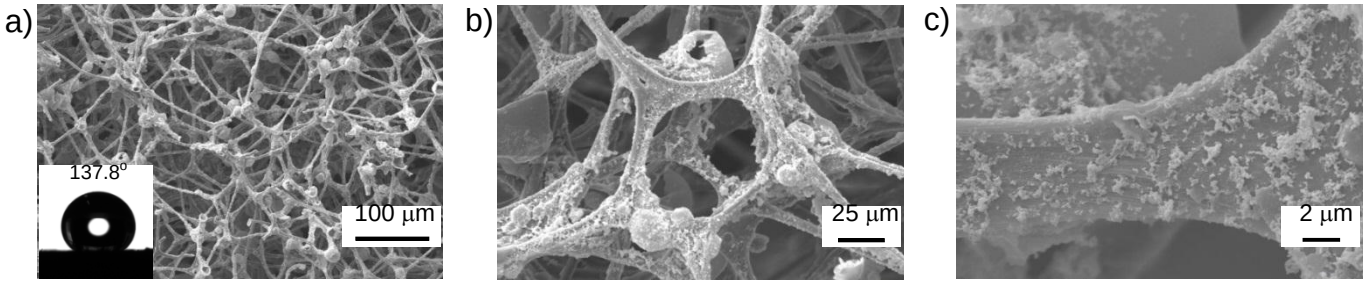

Fig. S6. SEM images in different magnifications of sponges after ultrasonication in ethanol for 2 min. Ultrasonication in ethanol was conducted to test the robustness of the immobilized carbon nanoparticles on the sponge surface. SEM observations showed that carbon nanoparticles anchored on the sponge were able to withstand sonication for 2 min maintaining the micro-nanoscale hierarchical porous structure. And the hydrophobicity was mostly retained with a water contact angle of 137.8^{o}.

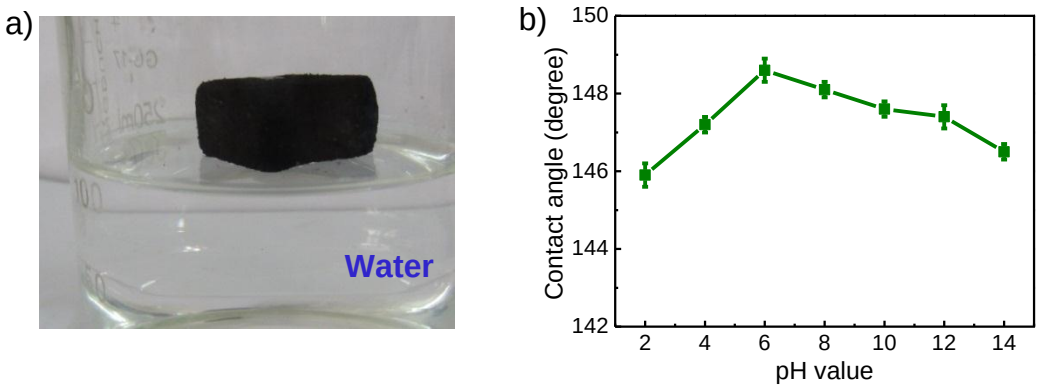

Fig. S7. a) A piece of UHF sponge floating on the water. b) Relationship between pH value and the water contact angle of the UHF sponges. Due to the ultralight density and hydrophobicity, the UHF sponge could float on the water. At the same time, the UHF sponge can repelled water of different pH values.

Fig. S8. Water contact angle of a glass slide blacken by a toluene burner. And the result came out to be 65.4^{o}. The Cassie equation, $\cos\theta_c=f_1(\cos\theta_1+1)-1$, was used to described the contact state between the water droplet and the surface of the sponge. Herein, θ_c (149^{o}) is the water contact angle of the UHF sponge; θ_1 is the water contact angle of the blacken glass slide (65.4^{o}); f_1 and f_2 are the fractional interfacial areas of the carbon particle on the skeleton surface and of the entrapped air on the sponge surface, respectively ($f_1+f_2=1$). 10.1 % of the contact area between the water droplet and the sponge is the carbon particles, and 89.9 % of the contact area between the water droplet and the sponge surface is occupied by air.

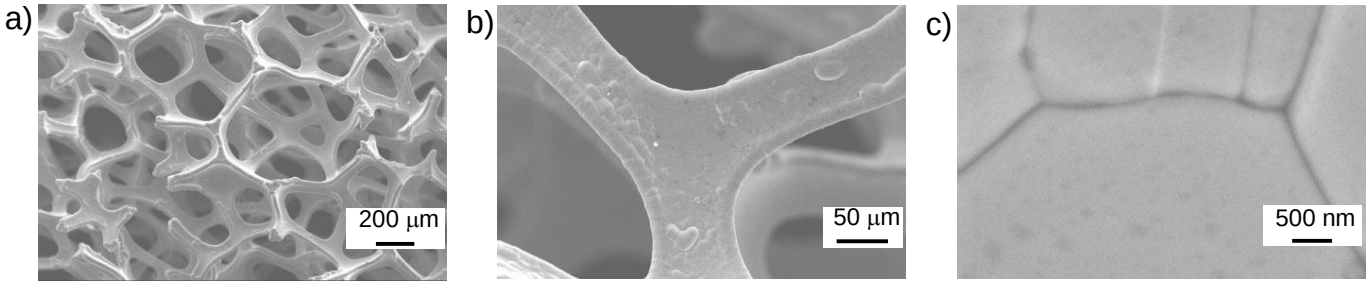

Fig. S9. SEM images of the original Nickel foam in different magnification times. The skeleton of the foam exhibits with smooth surface. The structure possesses pore of about 300-700 μm and the skeleton diameter is about 30-70 μm.

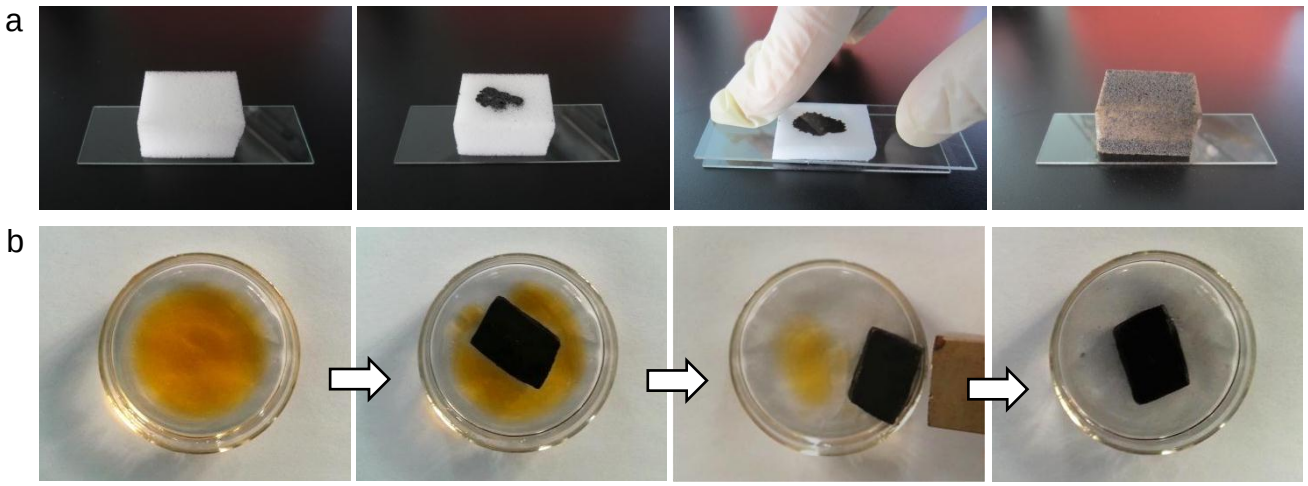

Fig. S10. (a) The PMF sponge was wetted by oleic acid-modified Fe_3O_4 nanoparticle toluene suspension by an absorb-compress-release cycle process. The oil-absorbed sponge was compressed from different direction to ensure the toluene and Fe_3O_4 nanoparticles could homogeneously distribute in the sponge. (b) Removal of toluene from the surface of water by a piece of obtained magnetic hydrophobic sponge under magnetic field; the toluene was dyed with Sudan I to aid observation.

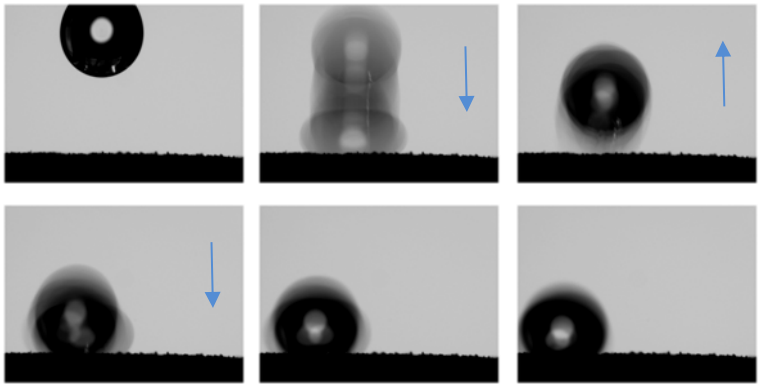

Fig. S11. Snapshots of a water droplet falling to an aclinic UHF sponge surface. The water droplet bounced immediately without any delay due to the low adhesion of the UHF sponge to the water droplets.

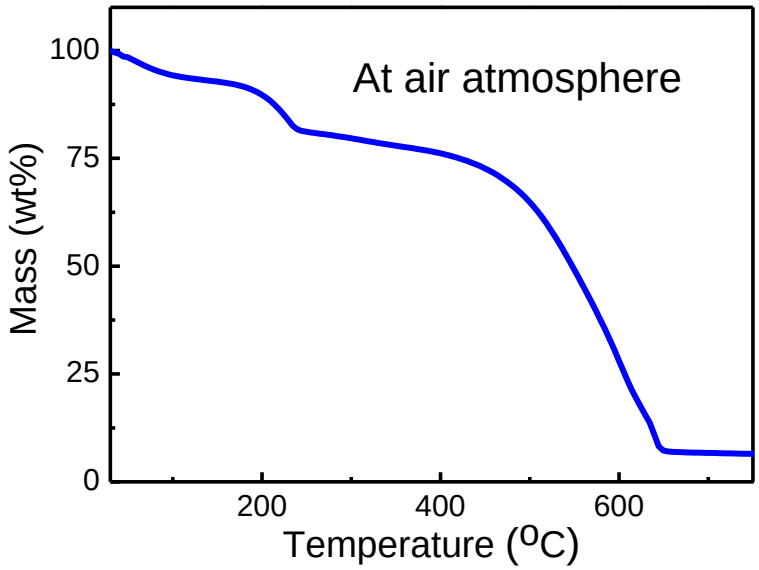

Fig. S12. TGA curve of the UHF sponge. TGA was performed under an air atmosphere and a heating rate of 10 ^{o}C min^{-1} form 30 to 800 ^{o}C. Before 100 ^{o}C, it loses ca. 5 % weight as the residual toluene in the sponge. The weight lost from 100 to 250 ^{o}C is attributed to evaporation of formaldehyde from the deformaldehyde reaction of PMF which is remnant in the UHF sponges.

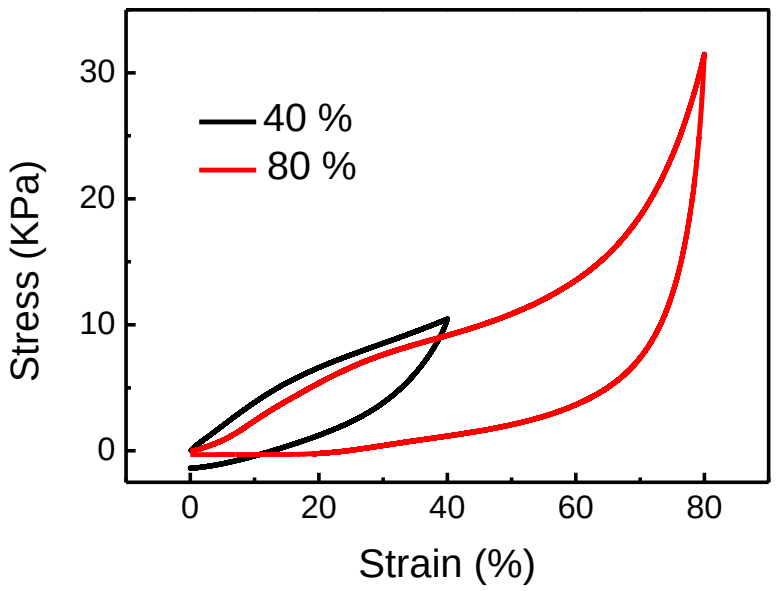

Fig. S13. Compressive stress-strain curves of UHF sponges at strain values of 40 and 80 %. The UHF sponges exhibited excellent compressibility in different strains.

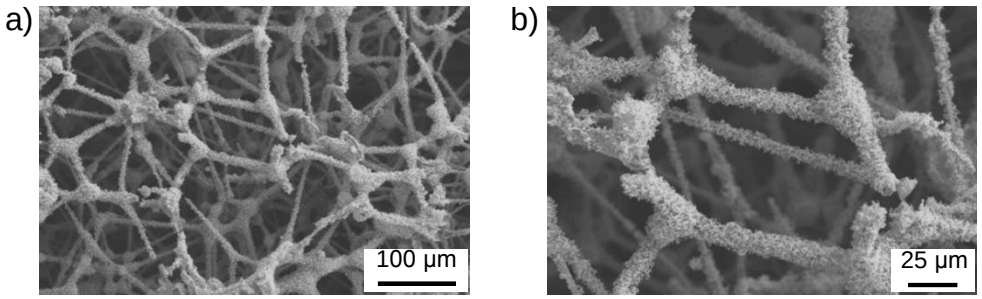

Fig. S14. (a,b) are the SEM images of the sponge after 1000 cycles compression testing with strain of 60% in different magnification. After 1000 cycles of compression testing with strain of 60%, the porous 3D interconnected structure is almost retained, with just some of the skeleton broken off.

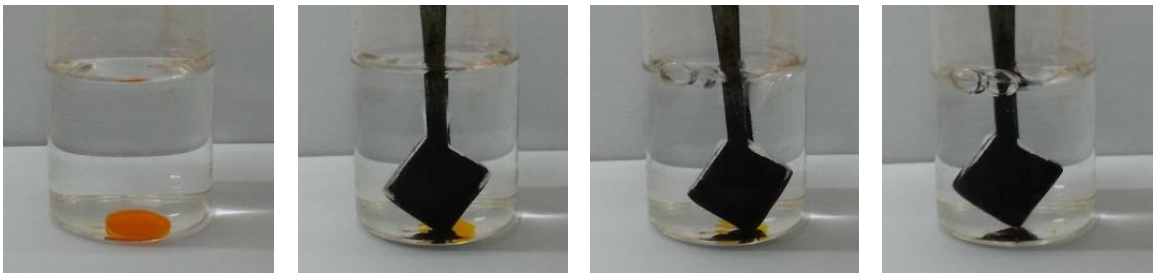

Fig. S15. Snapshots of removal process of dichloromethane (dyed by Sudan I) sinking below water using the UHF sponge. The oil was absorbed completely by the UHF sponge in several seconds.

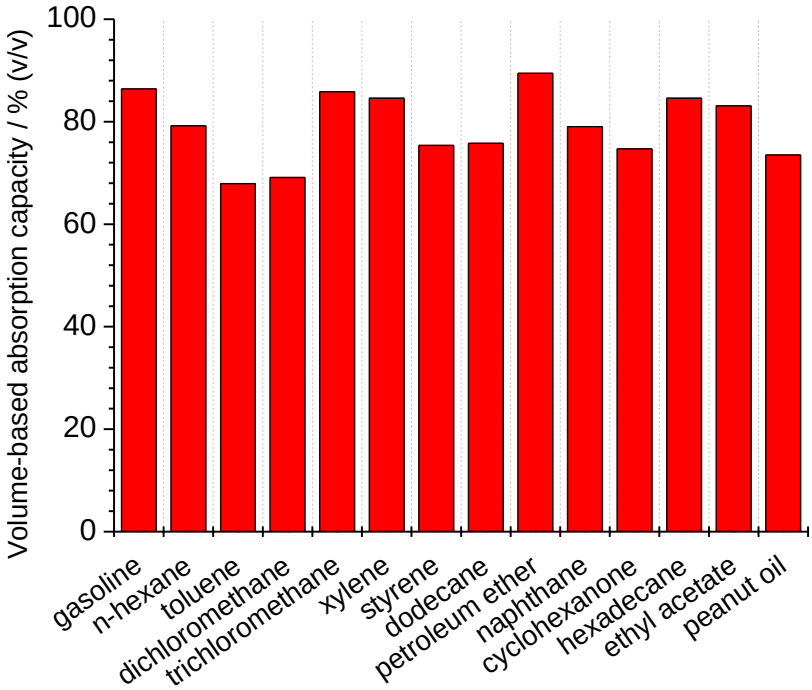

Fig. S16. Volume-based absorption capacities of the UHF sponges (with a density of 9 mg cm^{-3}) for oils and organic solvents.

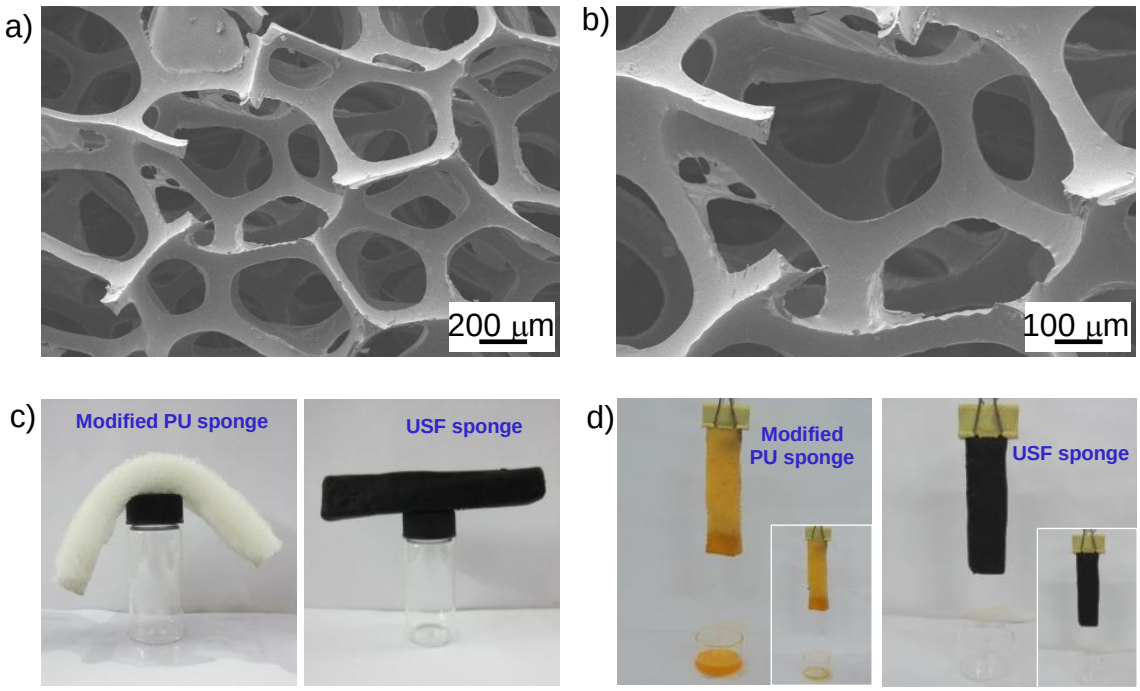

Fig. S17. a,b) are the SEM images of the modified PU sponges. The structure possesses pore of about 400-800 μm and the skeleton diameter is about 80-100 μm, which is much larger than the UHF sponges'. c) Hexane-absorbed sponges were putted on the top of a bottle. Modified PU sponge was distorted due to its own weight, and UHF sponge can be suspended horizontally. d) Hexane (dyed by Sudan I)-absorbed sponges were held vertically. Hexane flew out from modified PU sponge, while the UHF sponge did not.

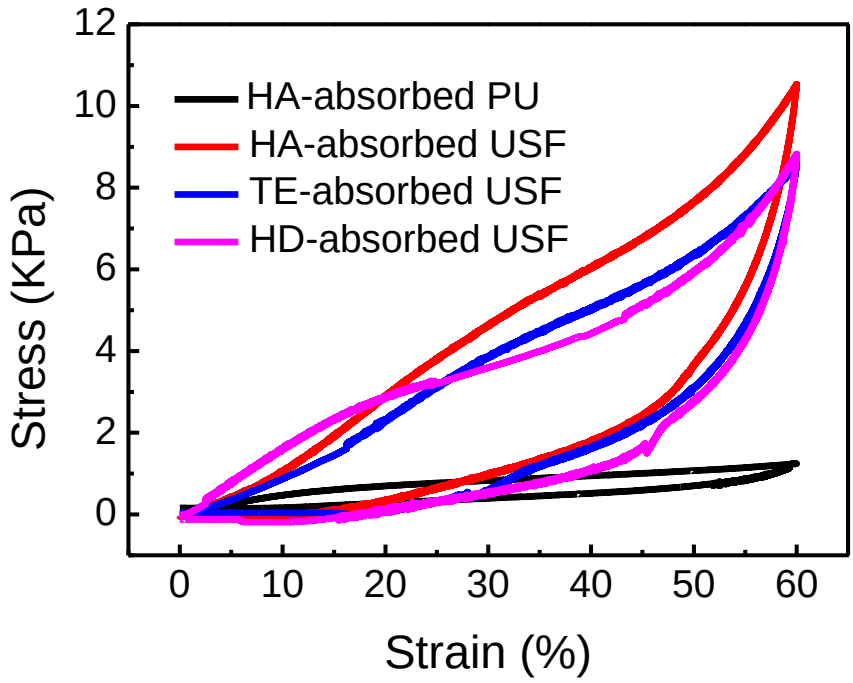

Fig. S18. Compressive stress–strain curves of oil-absorbed sponges, including hexane (HA)-absorbed modified PU sponge, HA-absorbed UHF sponge, toluene (TE)-absorbed UHF sponge, and hexadecane (HD)-absorbed UHF sponges.

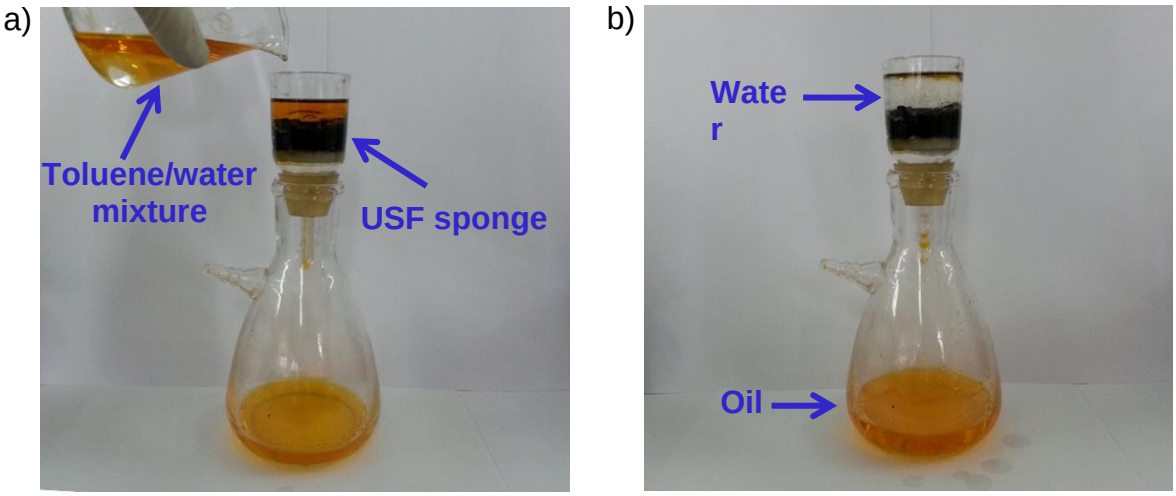

Fig. S19. Optical images of the oil/water separation process designed using the UHF sponge: a) the UHF sponge was fixed in the glass tube and the toluene (dyed by Sudan I)/water mixture was put into the glass tube; and b) the toluene successively penetrated through the foam dependent on its own weight, water was repelled and retained on the top due to the hydrophobicity of the sponge. The UHF sponge can be reused owing to its self-cleaning effect.

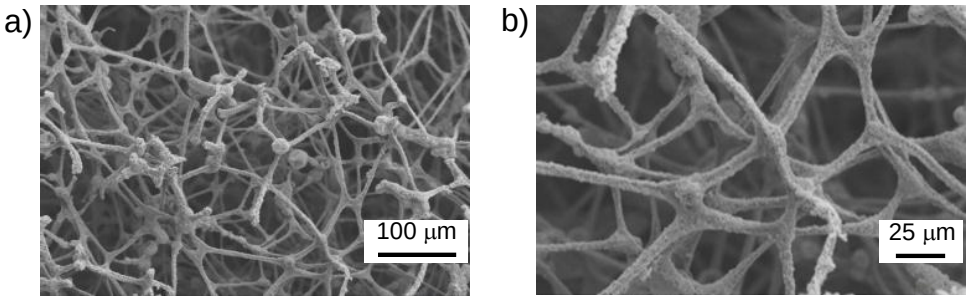

Fig. S20. SEM images of the UHF sponge after 5 cycles of absorption/distillation. Micaro-nanoscale hierarchical porous structure of the UHF sponge was maintained.

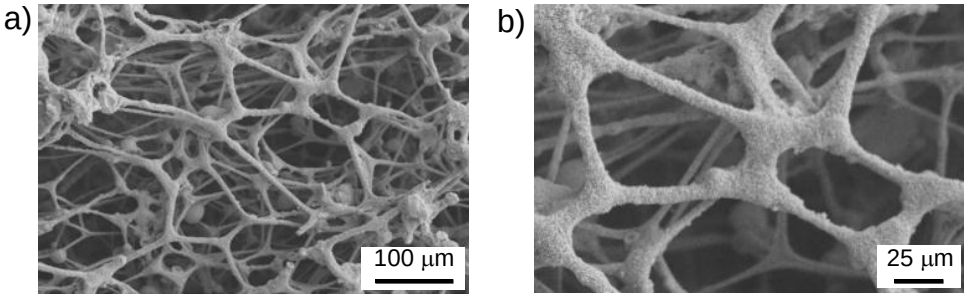

Fig. S21. SEM images of the UHF sponge after 5 cycles of absorption/combustion. Micaro-nanoscale hierarchical porous structure of the UHF sponge was maintained.

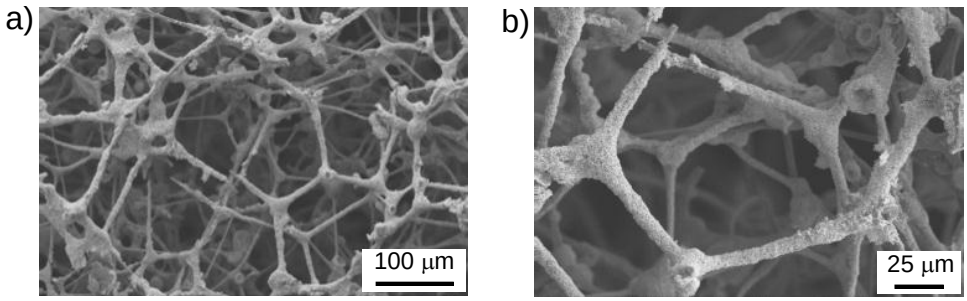

Fig. S22. SEM images of the UHF sponge after 5 cycles of absorption/squeezing. micaro-nanoscale hierarchical porous structure of the UHF sponge was maintained with some of the skeletons broken off.

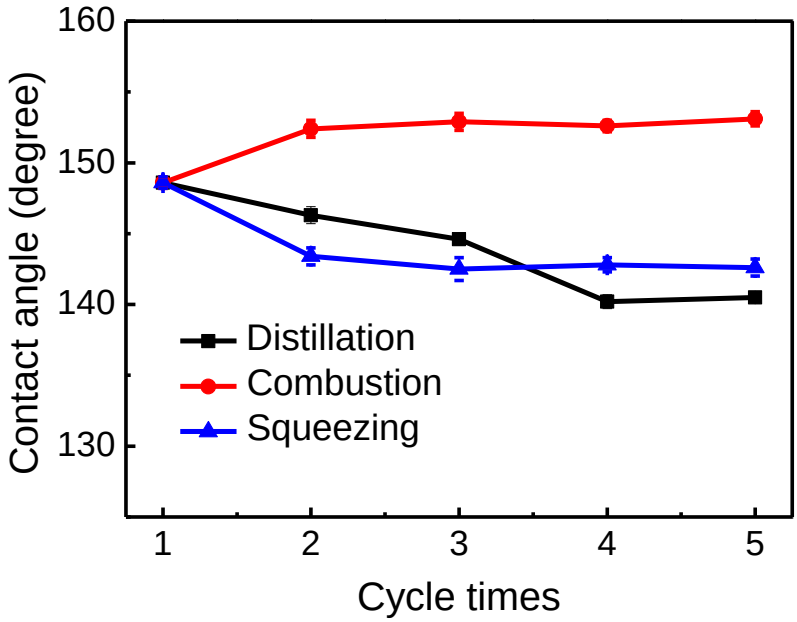

Fig. S23. Water contact angles recorded of the sponge after each oil-water separation process. It revealed that the three recycling methods of UHF sponges had little effect to the surface wettability of the sponges.